

A molecular crystal with an unprecedentedly long-lived photoexcited state

Toshio Naito,^{*a,b,c,d} Naoki Watanabe,^a Yuuka Sakamoto,^a Yuuko Miyaji,^a Takashi Shirahata,^{a,d} Yohji Misaki,^{a,d,e} Shunsuke Kitou^{f,g} and Hiroshi Sawa^f

^a Graduate School of Science and Engineering, Ehime University, Matsuyama 790-8577, Japan

^b Advanced Research Support Center (ADRES), Ehime University, Matsuyama 790-8577, Japan

^c Geodynamics Research Center (GRC), Ehime University, Matsuyama 790-8577, Japan

^d Research Unit for Development of Organic Superconductors, Ehime University, Matsuyama 790-8577, Japan

^e Research Unit for Power Generation and Storage Materials, Ehime University, Matsuyama 790-8577, Japan

^f Department of Applied Physics, Nagoya University, Nagoya, 464-8603, Japan

^g Institute for Molecular Science, Myodaiji, Okazaki 444-8585, Japan

**tnaito@ehime-u.ac.jp*

Table of Contents

1. Characterization of the sample	P. 2
2. X-ray structural analysis	P. 5
3. Theoretical calculation	P. 12
4. Electrical resistivity	P. 21
5. Magnetic susceptibility	P. 22
6. References	P. 23

1. Characterization of the sample.

IR spectra (450-4000 cm⁻¹, KBr pellets) were measured at 20°C using FT-IR FT-720 FREEEXACT-II (Horiba) with the resolution of 2 cm⁻¹.

Solution spectra in the UV-Vis (200-1100 nm) region were measured in CH₃CN with V-630 spectrophotometer (JASCO) at 20°C with the resolution of 2 nm.

Diffuse reflectance spectra (240-2600 nm, reference BaSO₄) was measured at 20°C using a UV-Vis-NIR spectrophotometer (Shimadzu UV-VIS SolidSpec-3700) with the resolution of 2.0 nm.

Table S1. Elemental analysis of BPY[Au(dmit)₂]₂

Run	C / %	H / %	N / %
#1	21.18	1.22	1.97
#2	21.38	1.39	1.89
Calculated*	21.14	0.88	2.05

*For C₂₄H₁₂Au₂N₂S₂₀

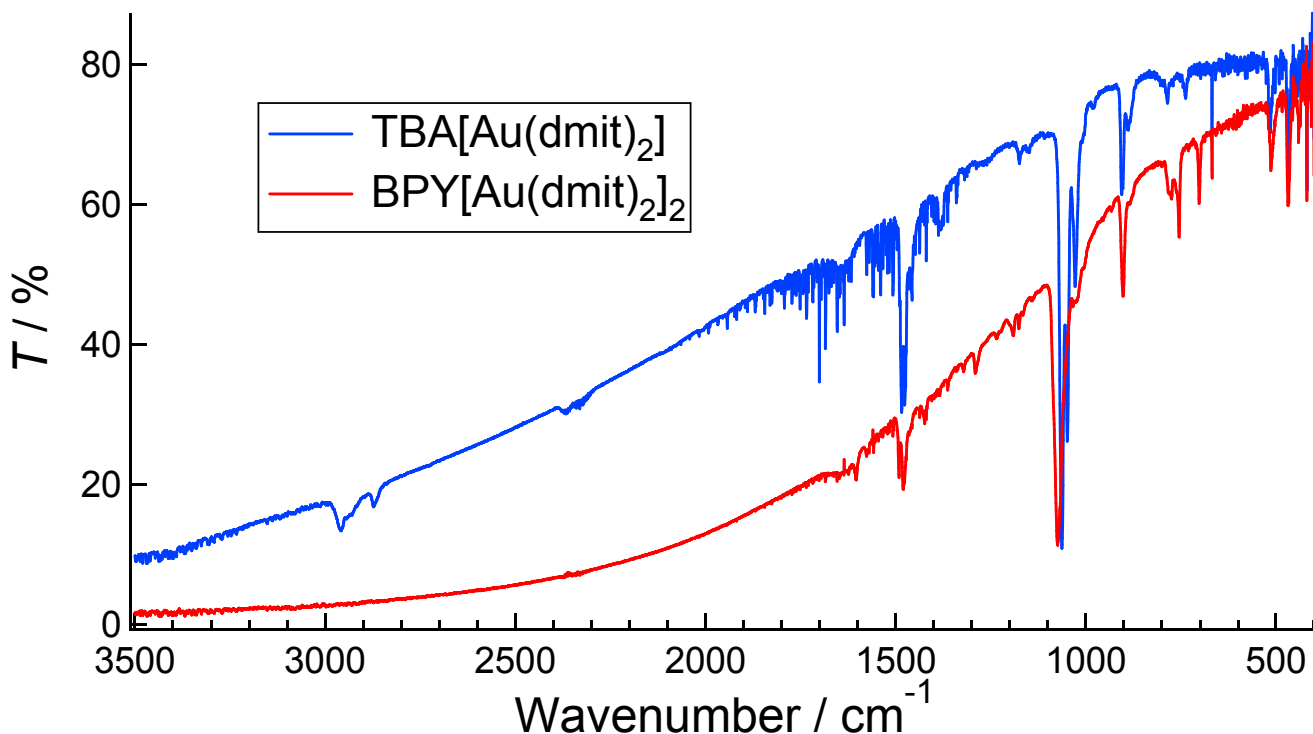


Figure S1. IR spectra (KBr disk, HORIBA FT-720). TBA = ⁿ(C₄H₉)₄N.

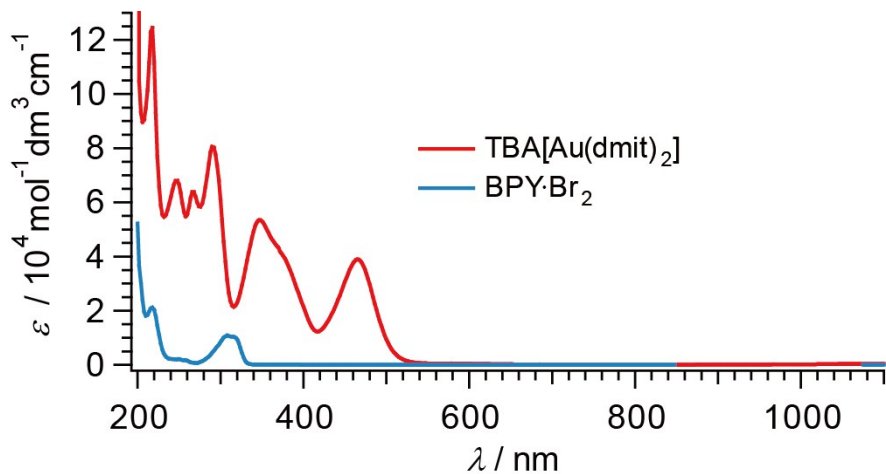


Figure S2. UV-Vis-NIR solution spectra of TBA[Au(dmit)₂] and BPY·Br₂ (CH₃CN, 20°C). TBA = ⁿ(C₄H₉)₄N.

Table S2. Assignment of IR peaks

BPY[Au(dmit) ₂] ₂	
Wavenumber / cm ⁻¹	Assignment
1603.52	BPY
1491.19	
1480.10	
1423.69	
1380.78	C=C
1369.57	
1321.00	
1290.14	BPY (C-N)
1233.25	BPY (C-C)
1190.83	
1171.54	
1074.16	C=S
1022.09	
902.04	BPY (C-C)
877.93	
776.21	C-S
754.51	
701.96	
513.45	Au-S
466.69	

ⁿ (C ₄ H ₉) ₄ N[Au(dmit) ₂]	
Wavenumber / cm ⁻¹	Assignment
2958.27	ⁿ (C ₄ H ₉) ₄ N (CH ₂ , antisymmetric stretch)
2868.11	ⁿ (C ₄ H ₉) ₄ N (CH ₂ , symmetric stretch)
1507.10	
1483.96	
1476.24	ⁿ (C ₄ H ₉) ₄ N (CH ₃ , bending)
1456.96	
1384.16	C=C
1171.54	ⁿ (C ₄ H ₉) ₄ N (C-N)
1063.07	
1048.60	C=S
1027.87	
905.90	
877.93	ⁿ (C ₄ H ₉) ₄ N (C-C)
784.89	
737.64	C-S
516.83	
466.21	Au-S
439.69	

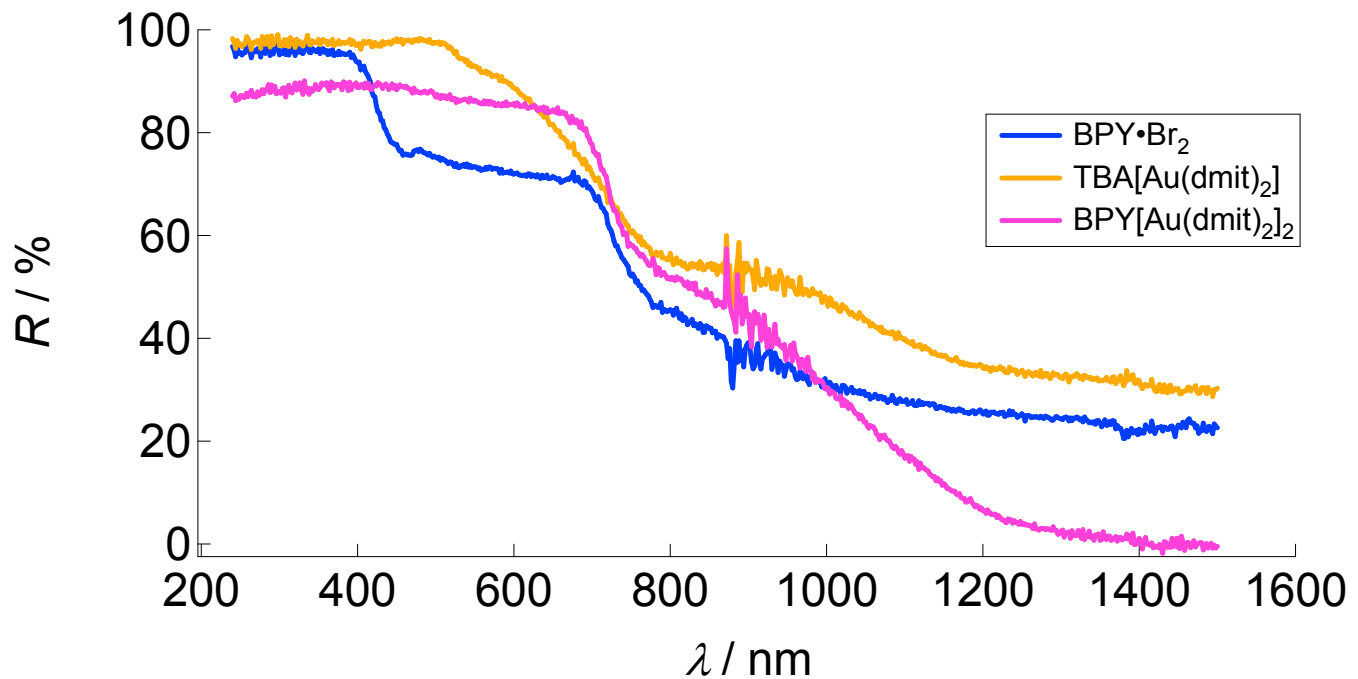


Figure S3. Diffuse reflectance spectra. TBA = ⁿ(C₄H₉)₄N. Measurement conditions; KBr disk, vs BaSO₄ powder, Shimadzu UV-VIS-NIR SolidSpec-3700, slit width = 2.0 nm, time constant = 1.0 s.

2. X-ray structural analysis

The structures were cross-checked using synchrotron radiation at BL02B1 at SPring-8, Japan. Four single crystals of high quality were selected by preliminary measurements of oscillation photographs. For these samples, data collection (1260 frames for each measurement composed of seven series of ω -scan, the exposure time was 1.5 sec for a frame, the oscillation angle in a series was 180° in total by the step of 1°) was carried out using the 44 keV radiation ($\lambda = 0.281532 \text{ \AA}$) and a pixel array X-ray detector PILATUS at 300 K under the dark condition. All the structures were solved by the direct method using SIR-92 program.^{S1} The peak intensities were averaged using SORTAV.^{S2} All the structures were refined by full-matrix least-squares on F^2 including all reflections by SHELLXL-97.^{S3} A helium gas flow system was utilized to control the temperature. The structure under the dark condition was also examined using a different single crystal at 300, 270, 240, 210, 180, 150, 100 and 30 K using the 35 keV radiation ($\lambda = 0.352195 \text{ \AA}$). The sample was cooled by 1 K/min from 300 K. After the data collection at 30 K under the dark condition was completed, it was irradiated with the UV-light source for 15 min, and the data collection of oscillation photographs was commenced with continuous UV-irradiation at 30 K using a UV-light source (Hg lamp; ASAHI SPECTRA, REX-1000, 1000 W, 360-450 nm, $\sim 8 \mu\text{Wcm}^{-2}$ at the crystal position, the distance between the crystal and the end of the quartz light guide was $\sim 10 \text{ cm}$). The transmission (%) property of the quartz guide was $\sim 60\text{-}65\%$ in the range of 360-450 nm. After the data collection under UV-irradiation at 30 K was completed, the UV-irradiation was continued until the sample was warmed up to 300 K by +20 K/min (13 min from 30 K to 300 K). Then the data collection was carried out under UV-irradiation at 300 K. The total time of UV-irradiation was 1 h 47 min. The effective temperature during UV-irradiation was corrected for heating effect of UV-irradiation based on the temperature-dependence of the unit cell volumes under dark conditions. Because of the limitation in the sample space in the equipment, we could not set the UV-irradiation condition (the light source, and the distance between the end of optical fiber and the crystal) to be identical with that in the measurements carried out at Ehime University. Considering the sample dependence found under the dark condition, the results obtained at SPring-8 serve as confirmation of semi-quantitative reproducibility.

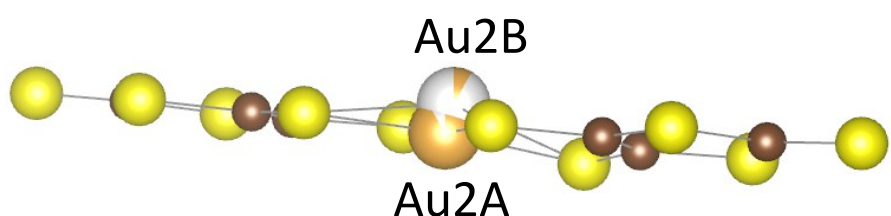
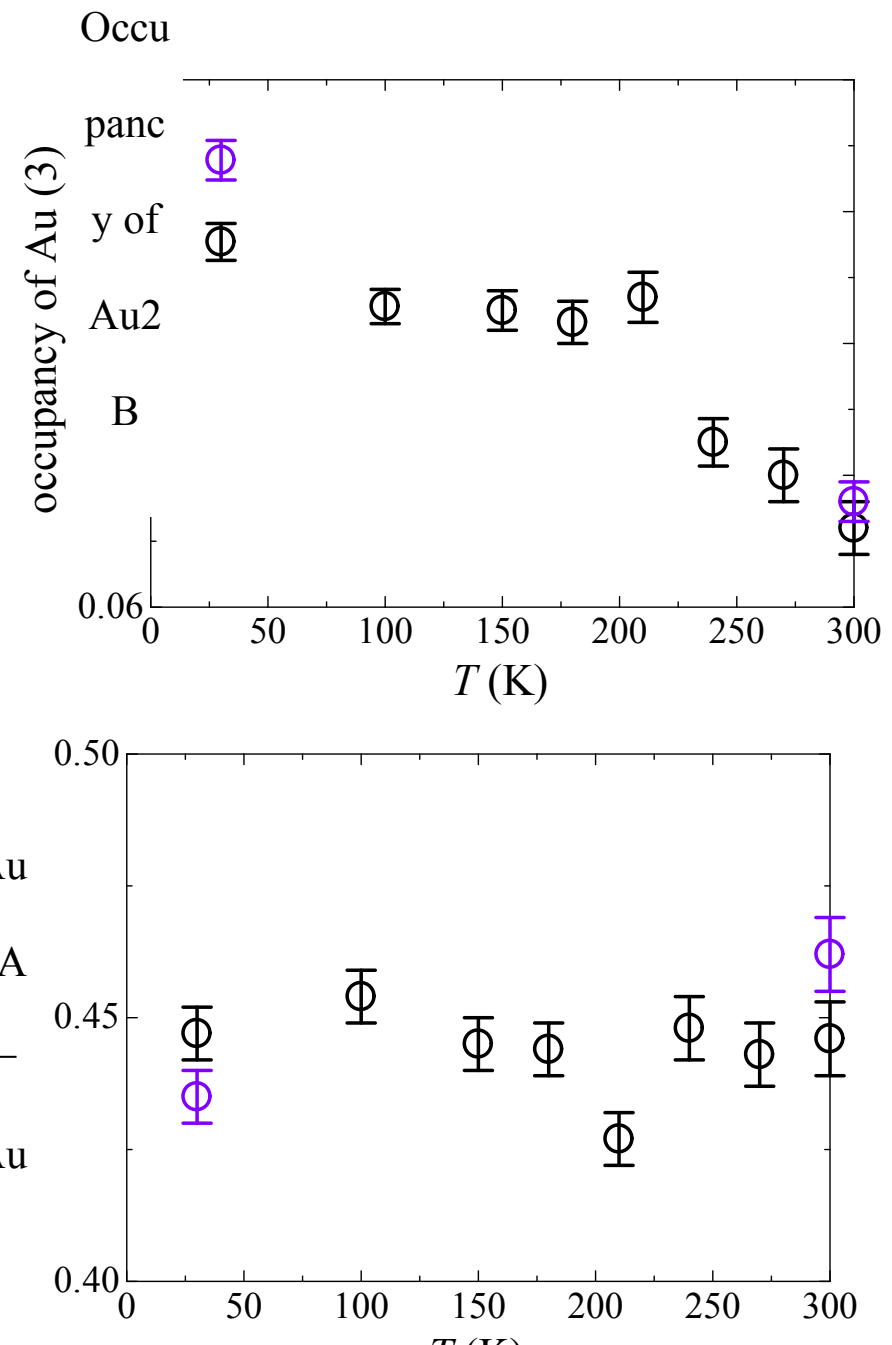


Figure S4. Occupancy of Au2B (upper), and interatomic distances between Au2A and Au2B (lower). The black and violet marks with error bars indicate the data under the dark and UV-irradiated conditions, respectively. Au2A and Au2B are located in the molecular plane and out of the molecular plane of Au(dmit)₂ anions, respectively.

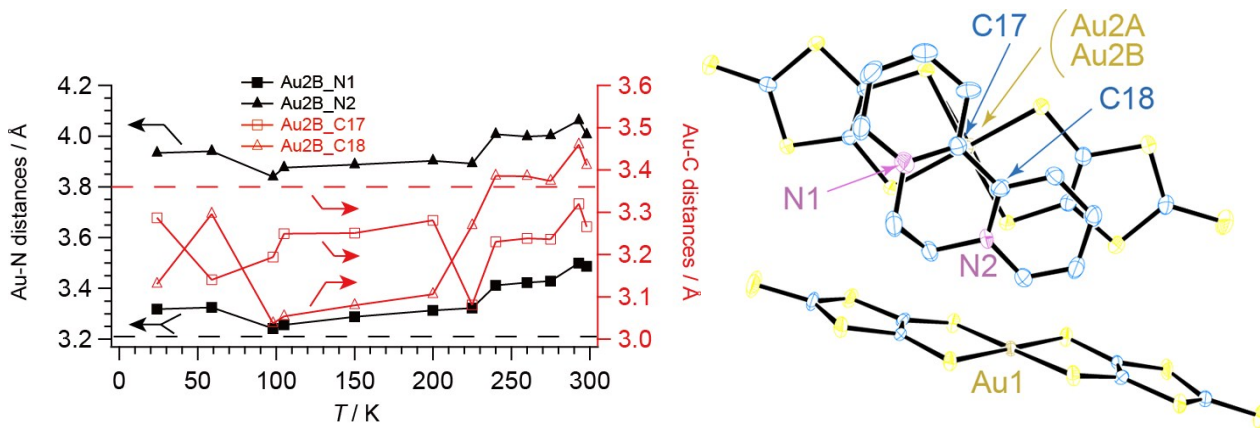


Figure S5. Interatomic distances between Au2B and N or C atoms on BPY. Horizontal broken lines indicate the van der Waals distances of Au-N (black; 3.21 Å) and Au-C (red; 3.36 Å), respectively. Each symbol includes uncertainty (esd) of the distance, which is in the order of 0.01 Å.

Table S3. Summary of crystallographic data.¹

Temperature (K) ²	300	298	293	275
Sample No.	Spring8-003	1	2	1
Cryst. dimension	0.06×0.12×0.02	0.29×0.11×0.03	0.19×0.15×0.02	0.29×0.11×0.03
<i>a</i> (Å)	11.2544(3)	11.270(2)	11.2630(3)	11.255(3)
<i>b</i> (Å)	14.4276(4)	14.443(3)	14.4291(3)	14.422(4)
<i>c</i> (Å)	23.5451(6)	23.561(5)	23.5623(5)	25.544(6)
β (°)	100.203(7)	100.176(3)	100.166(2)	100.265(4)
<i>V</i> (Å ³)	3762.65(17)	3774.8(13)	3769.11(15)	3760.7(17)
<i>D</i> _{calc} (g cm ⁻³)	2.407	2.399	2.403	2.408
μ (Cu $K\alpha$) (cm ⁻¹)	12.90	89.242	89.376	89.576
Abs. correc.	Empirical	Numerical	Empirical	Numerical
Trans. factors	0.010-0.100	0.429-0.765	0.336-0.836	0.442-0.764
CCDC deposit #	1892256	1584705	1584707	1584708
Reflection/Parameter	41.22	20.54	20.52	20.42
<i>R</i> _I , ³ <i>wR</i> ₂ , ⁴	0.0532, 0.1157	0.0434, 0.1050	0.0407, 0.0940	0.0699, 0.1566
GOF	1.205	1.057	1.033	1.134
Max Shift/Error	0.001	0.002	0.003	0.001

¹ For $C_{24}H_{12}Au_2N_2S_{20}$ (F.W. = 1363.51), Monoclinic, $P2_1/c$ (#14), $Z = 4$. ² “(UV)” designates the structure under UV irradiation, where the temperature indicated is corrected for actual sample temperature. ³ $I > 2.00\sigma(I)$. ⁴All reflections.

Table S3 (cont.). Summary of crystallographic data.¹

Temperature (K) ²	270	260	240	240	225
Sample No.	Spring8-003	2	2	Spring8-003	1
Cryst. dimension	0.06×0.12×0.02	0.19×0.15×0.02	0.19×0.15×0.02	0.06×0.12×0.02	0.29×0.11×0.03
<i>a</i> (Å)	11.2445(3)	11.2470(3)	11.2396(3)	11.2355(2)	11.236(4)
<i>b</i> (Å)	14.4064(4)	14.3967(3)	14.3805(3)	14.3863(3)	14.386(5)
<i>c</i> (Å)	23.5274(6)	23.5319(5)	23.5196(5)	23.5127(5)	23.509(8)
β (°)	100.330(7)	100.323(2)	100.412(2)	100.448(7)	100.431(4)
<i>V</i> (Å ³)	3749.49(17)	3748.60(15)	3738.90(15)	3737.51(13)	3737(2)
<i>D</i> _{calc} (g cm ⁻³)	2.415	2.416	2.422	2.423	2.423
μ (Mo $K\alpha$) (cm ⁻¹)	12.95	89.865	90.098	12.99	90.141
Abs. Correc.	Empirical	Empirical	Empirical	Empirical	Numerical
Trans. Factors	0.010-0.100	0.353-0.835	0.357-0.835	0.010-0.100	0.467-0.763
CCDC deposit #	1892039	1584709	1584710	1892257	1584711
Reflection/Parameter	41.10	20.38	20.32	40.96	20.28
<i>R</i> _I , ³ <i>wR</i> ₂ ⁴	0.0521, 0.1119	0.0374, 0.0858	0.0362, 0.0807	0.0513, 0.1113	0.0677, 0.1589
GOF	1.208	1.045	1.035	1.244	1.083
Max Shift/Error	0.003	0.002	0.003	0.001	0.001

¹ For C₂₄H₁₂Au₂N₂S₂₀ (F.W. = 1363.51), Monoclinic, *P*2₁/c (#14), *Z* = 4. ²“(UV)” designates the structure under UV irradiation, where the temperature indicated is corrected for actual sample temperature. ³*I* > 2.00 σ (*I*). ⁴All reflections.

Table S3 (cont.). Summary of crystallographic data.¹

Temperature (K) ²	210	200	180	150	150
Sample No.	Spring8-003	1	Spring8-003	Spring8-003	1
Cryst. dimension	0.06×0.12×0.02	0.29×0.11×0.03	0.06×0.12×0.02	0.06×0.12×0.02	0.29×0.11×0.03
<i>a</i> (Å)	11.2273(3)	11.224(3)	11.2193(2)	11.2105(2)	11.223(3)
<i>b</i> (Å)	14.3666(3)	14.366(4)	14.3461(3)	14.3252(3)	14.340(4)
<i>c</i> (Å)	23.4999(5)	23.531(7)	23.4863(4)	23.4734(5)	23.504(7)
β (°)	100.563(7)	100.582(3)	100.676(7)	100.788(7)	100.713(4)
<i>V</i> (Å ³)	3726.26(13)	3729.9(18)	3714.76(12)	3703.03 (13)	3716.7(18)
<i>D</i> _{calc} (g cm ⁻³)	2.430	2.428	2.438	2.446	2.437
μ (Mo $K\alpha$) (cm ⁻¹)	13.03	90.316	13.07	13.11	90.637
Abs. Correc.	Empirical	Numerical	Empirical	Empirical	Numerical
Trans. Factors	0.010-0.100	0.422-0.763	0.010-0.100	0.010-0.100	0.428-0.762
CCDC deposit #	1892258	1584712	1892259	1892261	1584713
Reflection/Parameter	40.88	20.30	40.76	40.59	20.23
<i>R</i> _I , ³ <i>wR</i> ₂ ⁴	0.0497, 0.1101	0.0596, 0.1288	0.0497, 0.1094	0.0493, 0.1088	0.0596, 0.1262
GOF	1.266	1.148	1.296	1.295	1.130
Max Shift/Error	0.002	0.002	0.001	0.001	0.001

¹ For C₂₄H₁₂Au₂N₂S₂₀ (F.W. = 1363.51), Monoclinic, *P*2₁/c (#14), *Z* = 4. ²“(UV)” designates the structure under UV irradiation, where the temperature indicated is corrected for actual sample temperature. ³*I* > 2.00 σ (*I*). ⁴All reflections.

Table S3 (cont.). Summary of crystallographic data.¹

Temperature (K) ²	105	100	98	59	30
Sample No.	1	Spring8-003	1	IMS-1	Spring8-003
Cryst. dimension	0.29×0.11×0.03	0.06×0.12×0.02	0.29×0.11×0.03	0.35×0.12×0.05	0.06×0.12×0.02
<i>a</i> (Å)	11.206(5)	11.1990(2)	11.186(4)	11.1908(17)	11.1847(2)
<i>b</i> (Å)	14.321(6)	14.2937(3)	14.295(5)	14.265(2)	14.2589(3)
<i>c</i> (Å)	23.452(10)	23.4589(4)	23.490(9)	23.468(4)	23.4445(4)
β (°)	100.990(6)	100.966(7)	101.019(4)	101.148(4)	101.159(7)
<i>V</i> (Å ³)	3694(3)	3686.62(12)	3687(2)	3675.7(10)	3668.27(12)
<i>D</i> _{calc} (g cm ⁻³)	2.451	2.457	2.456	2.464	2.469
μ (Mo $K\alpha$) (cm ⁻¹)	91.181	13.17	91.369	91.648	13.24
Abs. Correc.	Numerical	Empirical	Numerical	Numerical	Empirical
Trans. Factors	0.419-0.761	0.010-0.100	0.475-0.760	0.322-0.632	0.010-0.100
CCDC deposit #	1584714	1892042	1584715	1584717	1892043
Reflection/Parameter	16.31	40.39	19.92	19.90	40.24
<i>R</i> _I , ³ <i>wR</i> ₂ ⁴	0.0605, 0.1309	0.0490, 0.1159	0.0619, 0.1394	0.0323, 0.0799	0.0516, 0.1228
GOF	1.092	1.309	1.094	1.112	1.330
Max Shift/Error	0.001	0.001	0.001	0.004	0.001

¹ For C₂₄H₁₂Au₂N₂S₂₀ (F.W. = 1363.51), Monoclinic, *P*2₁/c (#14), *Z* = 4. ²“(UV)” designates the structure under UV irradiation, where the temperature indicated is corrected for actual sample temperature. ³*I* > 2.00 σ (*I*). ⁴All reflections.

Table S3 (cont.). Summary of crystallographic data.¹

Temperature (K) ²	24
Sample No.	IMS-1
Cryst. dimension	0.35×0.12×0.05
<i>a</i> (Å)	11.1886(17)
<i>b</i> (Å)	14.266(2)
<i>c</i> (Å)	23.468(4)
β (°)	101.137(4)
<i>V</i> (Å ³)	3675.3(10)
<i>D</i> _{calc} (g cm ⁻³)	2.464
μ (Mo $K\alpha$) (cm ⁻¹)	91.656
Abs. Correc.	Numerical
Trans. Factors	0.377-0.632
CCDC deposit #	1584742
Reflection/Parameter	15.35
<i>R</i> _I , ³ <i>wR</i> ₂ ⁴	0.0325, 0.0856
GOF	1.115
Max Shift/Error	0.002

¹ For C₂₄H₁₂Au₂N₂S₂₀ (F.W. = 1363.51), Monoclinic, *P*2₁/c (#14), *Z* = 4. ²“(UV)” designates the structure under UV irradiation, where the temperature indicated is corrected for actual sample temperature. ³*I* > 2.00 σ (*I*). ⁴All reflections.

Table S3 (cont.). Summary of crystallographic data.¹

Temperature (K) ²	305 (UV)	300 (UV)	300 (UV)
Sample No.	3	Spring8-003	3
Cryst. dimension	0.30×0.14×0.01	0.06×0.12×0.02	0.30×0.14×0.01
<i>a</i> (Å)	11.287(3)	11.2618(3)	11.272(3)
<i>b</i> (Å)	14.463(4)	14.4409(4)	14.442(4)
<i>c</i> (Å)	23.598(7)	23.5505(6)	23.582(7)
β (°)	100.111(4)	100.163(7)	100.156(3)
<i>V</i> (Å ³)	3792.6(18)	3769.94(17)	3778.8(18)
<i>D</i> _{calc} (g cm ⁻³)	2.388	2.402	2.397
μ (Mo Kα) (cm ⁻¹)	88.823	12.88	89.146
Abs. Correc.	Multi-scan	Empirical	Multi-scan
Trans. Factors	0.521-0.915	0.010-0.100	0.472-0.915
CCDC deposit #	1889084	1892044	1889085
Reflection/Parameter	25.46	41.26	25.51
<i>R</i> _I , ³ <i>wR</i> ₂ ⁴	0.0954, 0.2325	0.0637, 0.1350	0.1007, 0.2224
GOF	1.105	1.163	1.183
Max Shift/Error	0.001	0.001	0.001

¹ For C₂₄H₁₂Au₂N₂S₂₀ (F.W. = 1363.51), Monoclinic, *P*2₁/c (#14), *Z* = 4. ²“(UV)” designates the structure under UV irradiation, where the temperature indicated is corrected for actual sample temperature. ³*I* > 2.00σ(*I*). ⁴All reflections.

Table S3 (cont.). Summary of crystallographic data.¹

Temperature (K) ²	288 (UV)	250 (UV)	225 (UV)	200 (UV)
Sample No.	3	3	4	3
Cryst. dimension	0.30×0.14×0.01	0.30×0.14×0.01	0.22×0.11×0.01	0.30×0.14×0.01
<i>a</i> (Å)	11.269(3)	11.253(3)	11.2451(5)	11.2305(3)
<i>b</i> (Å)	14.435(4)	14.404(4)	14.3771(6)	14.3600(4)
<i>c</i> (Å)	23.580(6)	23.546(7)	25.5363(11)	23.5036(6)
β (°)	100.220(3)	100.391(5)	100.481(4)	100.564(2)
<i>V</i> (Å ³)	3774.8(17)	3753.8(18)	3741.7(3)	3726.18(17)
<i>D</i> _{calc} (g cm ⁻³)	2.399	2.412	2.420	2.430
μ (Mo Kα) (cm ⁻¹)	89.240	89.740	90.031	90.405
Abs. Correc.	Multi-scan	Multi-scan	Multi-scan	Multi-scan
Trans. Factors	0.481-0.915	0.521-0.914	0.551-0.914	0.263-0.914
CCDC deposit #	1889251	1889087	1889088	1889090
Reflection/Parameter	25.35	25.75	19.98	20.28
<i>R</i> _I , ³ <i>wR</i> ₂ ⁴	0.0926, 0.2190	0.0934, 0.2205	0.0474, 0.1124	0.0476, 0.1169
GOF	1.123	1.170	1.015	1.043
Max Shift/Error	0.001	0.000	0.002	0.004

¹ For C₂₄H₁₂Au₂N₂S₂₀ (F.W. = 1363.51), Monoclinic, *P*2₁/c (#14), *Z* = 4. ²“(UV)” designates the structure under UV irradiation, where the temperature indicated is corrected for actual sample temperature. ³*I* > 2.00σ(*I*). ⁴All reflections.

Table S3 (cont.). Summary of crystallographic data.¹

Temperature (K) ²	175 (UV)	150 (UV)	150 (UV)	125 (UV)
Sample No.	3	3	5	3
Cryst. dimension	0.30×0.14×0.01	0.30×0.14×0.01	0.279×0.091×0.010	0.30×0.14×0.01
<i>a</i> (Å)	11.2226(3)	11.2123(3)	11.1938(3)	11.2060(2)
<i>b</i> (Å)	14.3422(3)	14.3203(3)	14.3070(5)	14.3033(3)
<i>c</i> (Å)	23.4933(6)	23.4772(5)	23.4590(7)	23.4697(5)
β (°)	100.659(2)	100.762(2)	100.819(3)	100.850(2)
<i>V</i> (Å ³)	3716.16(16)	3703.28(15)	3690.2(2)	3694.54(13)
<i>D</i> _{calc} (g cm ⁻³)	2.437	2.445	2.454	2.451
μ (Mo Kα) (cm ⁻¹)	90.649	90.964	91.287	91.180
Abs. Correc.	Multi-scan	Multi-scan	Multi-scan	Multi-scan
Trans. Factors	0.263-0.913	0.271-0.913	0.676-0.913	0.311-0.913
CCDC deposit #	1889100	1889103	1889121	1889104
Reflection/Parameter	20.22	20.15	19.85	20.11
<i>R</i> _I , ³ <i>wR</i> ₂ ⁴	0.0487, 0.1209	0.0460, 0.1115	0.0472, 0.1221	0.0457, 0.1091
GOF	1.039	1.035	1.023	1.034
Max Shift/Error	0.001	0.002	0.001	0.003

¹ For C₂₄H₁₂Au₂N₂S₂₀ (F.W. = 1363.51), Monoclinic, *P*2₁/c (#14), *Z* = 4. ² “(UV)” designates the structure under UV irradiation, where the temperature indicated is corrected for actual sample temperature. ³*I* > 2.00σ(*I*). ⁴All reflections.

Table S3 (cont.). Summary of crystallographic data.¹

Temperature (K) ²	95 (UV)	30 (UV)
Sample No.	3	Spring8-003
Cryst. dimension	0.30×0.14×0.01	0.06×0.12×0.02
<i>a</i> (Å)	11.1996(2)	11.1857(2)
<i>b</i> (Å)	14.2837(3)	14.2553(3)
<i>c</i> (Å)	23.4641(5)	23.4488(4)
β (°)	100.955(2)	101.144(7)
<i>V</i> (Å ³)	3685.19(13)	3668.54(12)
<i>D</i> _{calc} (g cm ⁻³)	2.457	2.469
μ (Mo Kα) (cm ⁻¹)	91.411	12.88
Abs. Correc.	Multi-scan	Empirical
Trans. Factors	0.289-0.913	0.010-0.100
CCDC deposit #	1889105	1892262
Reflection/Parameter	20.04	40.25
<i>R</i> _I , ³ <i>wR</i> ₂ ⁴	0.0454, 0.1076	0.0512, 0.1198
GOF	1.029	1.343
Max Shift/Error	0.002	0.001

¹ For C₂₄H₁₂Au₂N₂S₂₀ (F.W. = 1363.51), Monoclinic, *P*2₁/c (#14), *Z* = 4. ² “(UV)” designates the structure under UV irradiation, where the temperature indicated is corrected for actual sample temperature. ³*I* > 2.00σ(*I*). ⁴All reflections.

3. Theoretical calculation

Molecular orbitals and band structures were calculated within the framework of an extended Hückel tight-binding approximation using CAESAR ver. 1.0 and 2.0 (Crystal and Electronic Structure Analyzer; PrimeColor Software, Inc.). The crystal structure (atomic parameters) observed at 100 K was utilized. The disorder at one of the Au sites (Au2) was ignored and all of the Au2 atoms were assumed to be the P-geometry Au atoms (Au2A) in the band calculation (**Figs. S6(a)** and **S6(b)**). Similar band calculations were also carried out based on different assumption (all Au2 sites were occupied with Au2B) and/or different structure (at 298 K) (**Figs. S6(c) – S6(e)**). The parameter set utilized in the calculation is summarized in Supporting Information Table S4 (see below). Additionally, molecular orbitals and spin distribution were also calculated using Gaussian 09 (B3LYP/ LanL2DZ(5d,7f))^{S4} with the aid of GaussView 5.0.^{S5} For the open-shell molecules [Au(C₃S₅)₂]⁰, unrestricted method was utilized.

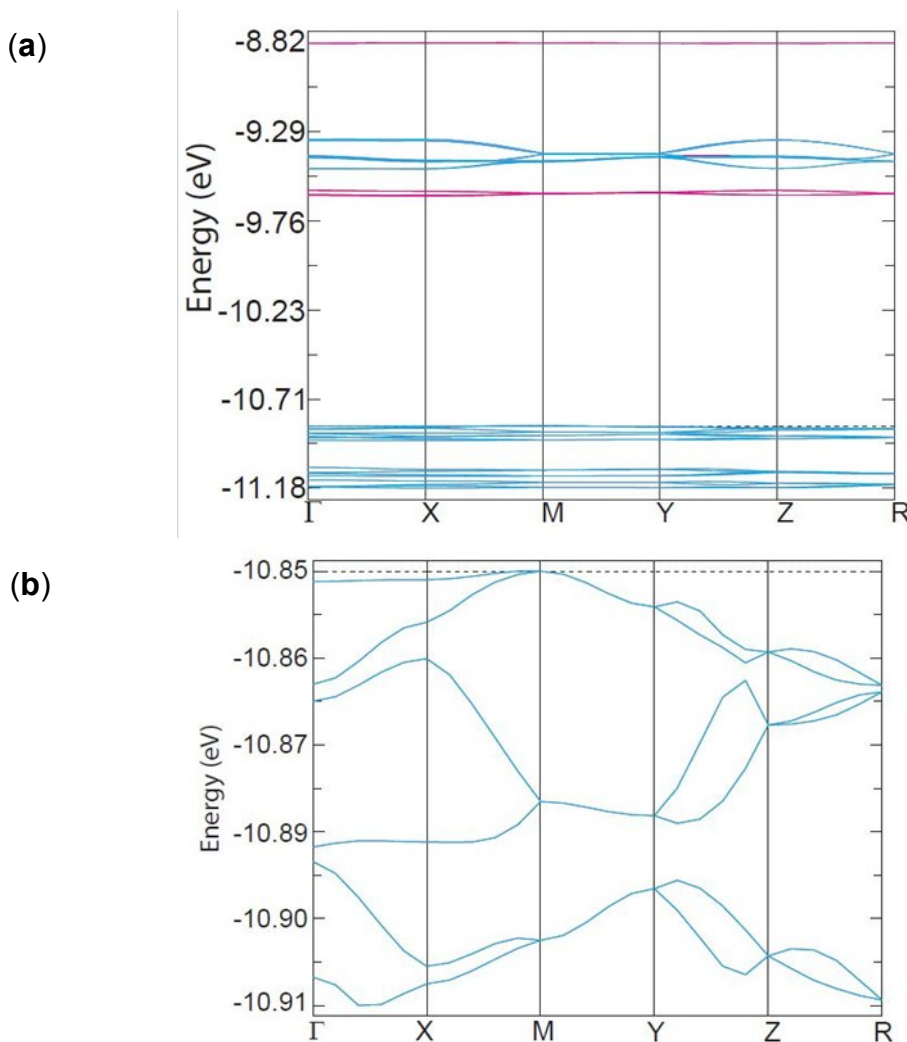
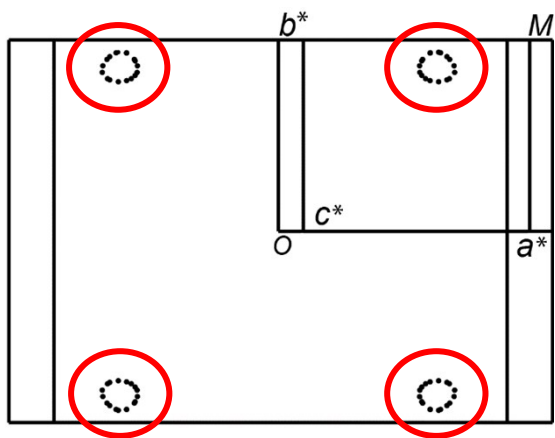
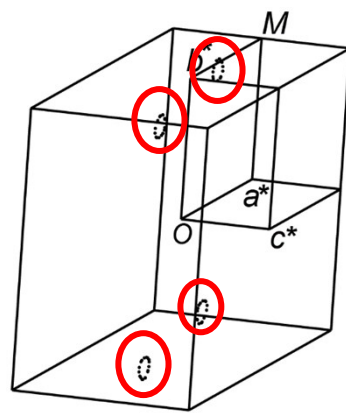


Figure S6. (a) Tight-binding band structure based on the observed structure at 100 K. Contributions of Au(dmit)₂ and BPY to each band are described by cyan and magenta, respectively. For quantitative information, see **Tables S4-S8**. Qualitatively the same band structures were obtained from the similar calculation based on different assumption on the Au2 sites and the structure at different temperatures, except for the Fermi surface (see **Figs. S6(c)-S6(e)**). (b) Expanded view around the Fermi level (-10.85 eV).

(c)



(d)



(e)

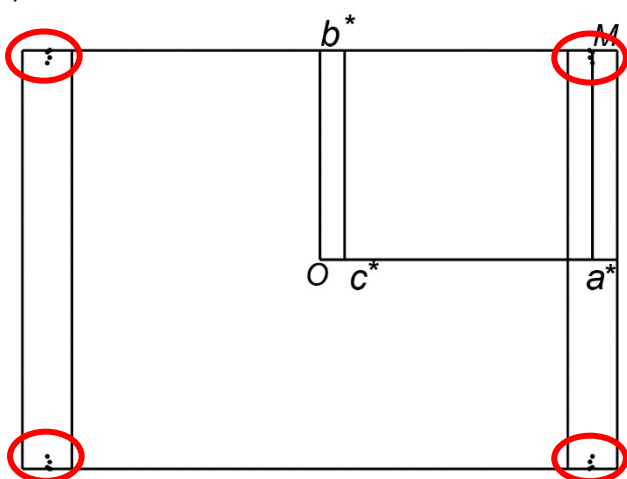


Figure S6 (cont). Fermi surfaces (hole pockets; black dotted ovals encircled by red) from tight-binding band calculation based on (c), (d) the observed structure at 98 K with assumption that all the Au2 sites were occupied with Au2A (square-planar coordinate Au(III)), and (e) the observed structure at 98 K with assumption that all the Au2 sites were occupied with Au2B (non-planar coordinate Au(III)). No Fermi surfaces appeared by the same calculation based on the observed structure at 298 K, whether the Au2 sites were assumed to be occupied by Au2A or Au2B only.

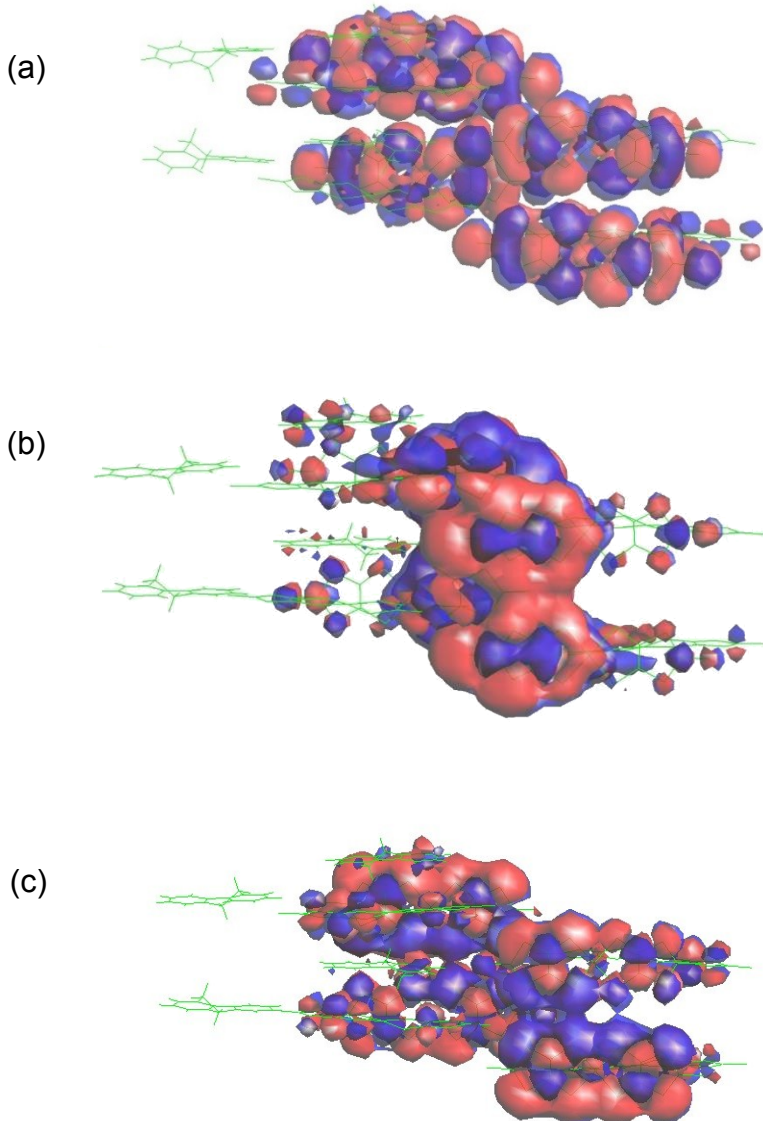


Figure S7. Overlap of molecular orbitals. Selected pairs of molecular orbitals (MOs) in the solid state of $\text{BPY}[\text{Au}(\text{dmit})_2]_2$ neighboring and interacting with each other. Molecules are shown by wireframes of green thin lines. Calculated by a tight-binding method. (a) MO#520 (around the Fermi level E_F). (b) MO#541 (2.76 eV = excitation wavelength of 450 nm above E_F). (c) MO#564 (4.43 eV = excitation wavelength of 280 nm above E_F). Blue and red designate lobes of different phases from each other. These calculated results illustrate there is a close intermolecular network among the $\text{Au}(\text{C}_3\text{S}_5)_2$ radical anions in UV-excited states (b). In addition, involvement of the BPY cations in the intermolecular interaction is also shown, particularly in the UV-excited states (b and c). Note here that the lobes of the BPY cations at the left-hand side are not shown in these figures in order to show the molecular arrangement (wireframes).

Table S4. Molecular orbital contribution in calculated band structures. MO# indicates the serial number beginning with the most stable molecular orbital. The unpaired electron lies in MO520. The green-colored cells show the coefficient of each atomic orbital in the given MO, while the yellow-colored cells show (sub)total contribution of each molecular species ($dmit = [Au(dmit)_2]^{δ-}$, $BPY = BPY^{2δ+}$), which was estimated from the square sum of the coefficients involved. The bottom two rows show the contribution from $BPY^{2δ+}$ and $[Au(dmit)_2]^{δ-}$ in the given MO by %. For showing the relative contribution from Au(III) and dmit ligands to the MO of $[Au(dmit)_2]^{δ-}$, the coefficients of Au, S and C atomic orbitals are separately shown. The calculation was performed based on the atomic parameters obtained from the X-ray structural analysis at the temperature indicated. In the calculation, it was assumed that all the Au2 sites were occupied either by the square-planar coordinate Au(III) (Au2A) only or by the non-planar coordinate Au(III) (Au2B) only.

(98 K, Au2A)

MO#	517	518	519	520	521	522	523	524	525	526	527	528
energy level [eV]	-10.923	-10.917	-10.913	-10.906	-9.649	-9.647	-9.635	-9.629	-9.418	-9.415	-9.411	-9.41
Au(6s)	4.55E-05	2.77E-05	6.22E-05	3.33E-05	1.51E-06	1.62E-06	2.06E-06	3.4E-06	8.06E-06	2.23E-05	2.39E-05	2.27E-05
Au(5p)	6.7E-05	0.000116	5.3E-05	8.11E-05	0.000702	0.000707	2.62E-05	0.000462	0.001341	0.003184	0.002887	0.003008
Au(5d)	0.02267	0.022525	0.022784	0.022628	0.007988	0.009145	0.001309	0.008454	0.45003	0.445753	0.438655	0.437283
S(3p)	0.565913	0.573379	0.566903	0.573754	0.018868	0.021681	0.005123	0.021884	0.874518	0.881164	0.86705	0.865972
S(3s)	0.000249	0.000264	0.0002	0.000238	0.001034	0.001382	0.000169	0.001231	0.079694	0.076566	0.075977	0.06014
C(2p)	0.546251	0.540245	0.543562	0.538131	0.821374	0.819662	0.83888	0.826088	0.009971	0.007523	0.021099	0.023186
C(2s)	0.000065	7E-05	0.000141	0.00013	0.0004	0.000388	0.000386	0.000395	0.000558	0.000585	0.000563	0.000581
dmit	1.134067	1.134848	1.128479	1.129623	0.030477	0.034796	0.010302	0.037272	1.413339	1.413818	1.391064	1.388384
BPY	0.002462	0.003476	0.009915	0.010484	1.218379	1.214615	1.238573	1.213684	0.004133	0.001481	0.022808	0.025031
total	1.136528	1.138323	1.138394	1.140107	1.248855	1.249411	1.248875	1.250956	1.417472	1.415298	1.413872	1.413415
dmit%	99.7834%	99.6947%	99.1290%	99.0805%	2.4404%	2.7850%	0.8249%	2.9795%	99.7085%	99.8954%	98.3869%	98.2290%
BPY%	0.2166%	0.3053%	0.8710%	0.9195%	97.5596%	97.2150%	99.1751%	97.0205%	0.2915%	0.1046%	1.6131%	1.7710%

(98 K, Au2B)

MO#	517	518	519	520	521	522	523	524	525	526	527	528
energy level [eV]	-10.945	-10.942	-10.939	-10.928	-10.076	-10.073	-10.072	-10.07	-9.643	-9.64	-9.64	-9.63
Au(6s)	0.000196	0.0001792	0.0001806	0.0001676	0.0022342	0.0021947	0.002182	0.0021141	0.0001253	3.26E-06	0.0001515	0.0002846
Au(5p)	5.177E-05	5.657E-05	5.131E-05	5.815E-05	0.0028181	0.0027063	0.0026968	0.0026062	0.0012947	5.153E-05	0.0013041	0.0025904
Au(5d)	0.0237222	0.0232482	0.0239127	0.0234357	0.3776574	0.3768765	0.3776854	0.3767518	0.004873	0.0015368	0.0021386	0.0062318
S(3p)	0.5655925	0.5676936	0.5685159	0.5752175	0.8761938	0.8748123	0.8783046	0.8767754	0.0136226	0.0067797	0.0067687	0.0184623
S(3s)	0.0003619	0.000371	0.0003471	0.0003606	0.0622001	0.054766	0.0587976	0.0586629	0.0007253	0.0005286	0.0001525	0.0009072
C(2p)	0.5439123	0.5431022	0.5421765	0.5375882	0.0217429	0.0234867	0.0211493	0.0230507	0.825696	0.8353905	0.8334887	0.8238748
C(2s)	0.0001792	0.0001258	0.0001503	0.0001774	0.0004218	0.0004253	0.0004178	0.0004229	0.0003977	0.0003771	0.0003801	0.0003867
dmit	1.1323678	1.1346141	1.1344821	1.1355575	1.3400895	1.3383102	1.3427962	1.3402868	0.023113	0.0100693	0.0145437	0.0349648
BPY	0.0021717	0.0002399	0.0010959	0.0019943	0.0053266	0.0073541	0.003277	0.0057565	1.2240941	1.2385162	1.2319717	1.2116409
total	1.1345395	1.134854	1.135578	1.1375518	1.3454161	1.3456644	1.3460732	1.3460433	1.2472071	1.2485854	1.2465154	1.2466057
dmit%	99.8086%	99.9789%	99.9035%	99.8247%	99.6041%	99.4535%	99.7566%	99.5723%	1.8532%	0.8065%	1.1667%	2.8048%
BPY%	0.1914%	0.0211%	0.0965%	0.1753%	0.3959%	0.5465%	0.2434%	0.4277%	98.1468%	99.1935%	98.8333%	97.1952%

Table S4 (cont). Molecular orbital contribution in calculated band structures. MO# indicates the serial number beginning with the most stable molecular orbital. The unpaired electron lies in MO520. The green-colored cells show the coefficient of each atomic orbital in the given MO, while the yellow-colored cells show (sub)total contribution of each molecular species ($dmit = [Au(dmit)_2]^{δ-}$, BPY = $BPY^{2δ+}$), which was estimated from the square sum of the coefficients involved. The bottom two rows show the contribution from $BPY^{2δ+}$ and $[Au(dmit)_2]^{δ-}$ in the given MO by %. For showing the relative contribution from Au(III) and dmit ligands to the MO of $[Au(dmit)_2]^{δ-}$, the coefficients of Au, S and C atomic orbitals are separately shown. The calculation was performed based on the atomic parameters obtained from the X-ray structural analysis at the temperature indicated. In the calculation, it was assumed that all the Au2 sites were occupied by either the square-planar coordination Au(III) (Au2A) only or the non-planar coordination Au(III) (Au2B) only.

(298 K, Au2A)

MO#	517	518	519	520	521	522	523	524	525	526	527	528
energy level [eV]	-10.912	-10.907	-10.905	-10.894	-9.623	-9.62	-9.614	-9.606	-9.484	-9.455	-9.454	-9.42
Au(6s)	0.000124	0.000126	9E-05	8.93E-05	2.7E-07	1.5E-07	2.61E-06	1.59E-06	1.2E-07	2.9E-07	2.6E-07	9.9E-07
Au(5p)	5.06E-05	4.69E-05	3.95E-05	4.65E-05	8.76E-06	0.000551	0.000156	0.000394	0.001228	0.001231	0.001221	0.001256
Au(5d)	0.022596	0.022638	0.022449	0.022447	5.58E-05	0.005407	0.000356	0.005723	0.445219	0.443451	0.443255	0.439797
S(3p)	0.569303	0.573903	0.572939	0.578525	0.000293	0.013608	0.002743	0.015368	0.8752	0.884299	0.884441	0.893212
S(3s)	0.000292	0.000287	0.000339	0.000332	2.62E-05	0.000803	7.46E-05	0.000856	0.079444	0.076507	0.07649	0.073026
C(2p)	0.545006	0.541796	0.542896	0.538675	0.842209	0.831763	0.842667	0.835006	0.008952	0.007589	0.007741	0.008147
C(2s)	0.00012	9.69E-05	8.74E-05	0.000122	0.000419	0.000439	0.000431	0.000434	0.000585	0.000631	0.000634	0.000717
dmit	1.136409	1.138305	1.138638	1.138845	0.000482	0.021891	0.005853	0.02644	1.409301	1.413702	1.413708	1.415479
BPY	0.00151	0.000765	0.000316	0.002255	1.249433	1.229194	1.244668	1.22599	0.001862	1.07E-05	0.000137	0.000943
total	1.137919	1.13907	1.138953	1.1411	1.249915	1.251085	1.250522	1.25243	1.411163	1.413713	1.413845	1.416422
dmit%	99.8673%	99.9328%	99.9723%	99.8024%	0.0385%	1.7498%	0.4681%	2.1111%	99.8681%	99.9992%	99.9903%	99.9335%
BPY%	0.1327%	0.0672%	0.0277%	0.1976%	99.9615%	98.2502%	99.5319%	97.8889%	0.1319%	0.0008%	0.0097%	0.0665%

(298 K, Au2B)

MO#	517	518	519	520	521	522	523	524	525	526	527	528
energy level [eV]	-10.913	-10.908	-10.907	-10.897	-9.696	-9.692	-9.691	-9.687	-9.623	-9.614	-9.612	-9.601
Au(6s)	0.000125	0.000105	0.000117	0.0001	0.000908	0.000924	0.000871	0.000907	4.5E-07	1.57E-05	3.56E-05	2.53E-05
Au(5p)	4.83E-05	4.38E-05	5.19E-05	5.29E-05	0.002565	0.002781	0.00197	0.001725	6.82E-06	0.000872	4.66E-05	0.000811
Au(5d)	0.022551	0.022261	0.022588	0.022281	0.382673	0.406551	0.402732	0.416368	5.63E-05	0.011787	0.022736	0.028591
S(3p)	0.568789	0.571639	0.573878	0.577889	0.811842	0.861267	0.853629	0.883645	0.00031	0.025914	0.050203	0.063992
S(3s)	0.000303	0.000324	0.000295	0.000316	0.064322	0.054251	0.067922	0.070283	2.59E-05	0.001405	0.004329	0.00512
C(2p)	0.545551	0.544062	0.541898	0.53955	0.078721	0.032036	0.041341	0.014299	0.842196	0.819749	0.799203	0.788541
C(2s)	0.000121	9.34E-05	9.97E-05	0.000121	0.000505	0.000498	0.000502	0.000494	0.000418	0.000436	0.000421	0.000426
dmit	1.136482	1.138453	1.138372	1.139379	1.275829	1.353977	1.340436	1.386396	0.000493	0.043443	0.078871	0.102782
BPY	0.001297	0.000118	0.000704	0.001283	0.098337	0.028915	0.042336	0.001944	1.249453	1.209564	1.179967	1.157562
total	1.137779	1.138571	1.139076	1.140661	1.374167	1.382892	1.382772	1.388339	1.249946	1.253007	1.258839	1.260344
dmit%	99.8860%	99.9897%	99.9382%	99.8876%	92.8439%	97.9091%	96.9383%	99.8600%	0.0394%	3.4671%	6.2654%	8.1551%
BPY%	0.1140%	0.0103%	0.0618%	0.1124%	7.1561%	2.0909%	3.0617%	0.1400%	99.9606%	96.5329%	93.7346%	91.8449%

Table S5. Parameters utilized in tight-binding band calculation.

Atoms	Atomic orbitals	H_{ii} / eV ^a	ζ_1	c_1 ^b	ζ_2	c_2 ^b
Au	6s	-10.9200	2.60200	1.00000	NA	NA
	6p	-5.5500	2.58400	1.00000	NA	NA
	5d	-15.0760	6.16300	0.68510	2.79400	0.56900
S	3s	-20.0000	2.12200	1.00000	NA	NA
	3p	-13.3000	1.82700	1.00000	NA	NA
N	2s	-26.0000	1.95000	1.00000	NA	NA
	2p	-13.4000	1.95000	1.00000	NA	NA
C	2s	-21.4000	1.62500	1.00000	NA	NA
	2p	-11.4000	1.62500	1.00000	NA	NA
H	1s	-13.6000	1.30000	1.00000	NA	NA

^a $H_{ii} = -\text{VSIP}$ (valence-state ionization potential [eV]). The double-zeta (for Au 5d) or single-zeta (for the remaining orbitals) Slater type orbitals (STO's) are used;

$$\chi_\mu(r, \theta, \phi) \propto r^{n-1} \exp(-\zeta r) Y(\theta, \phi) \text{ (single-zeta STO)}$$

$$\chi_\mu(r, \theta, \phi) \propto r^{n-1} [c_1 \exp(-\zeta_1 r) + c_2 \exp(-\zeta_2 r)] Y(\theta, \phi)$$

(double-zeta STO)

^b c_1 and c_2 correspond to 1 and 0 in single-zeta STO, and c_1 and c_2 in double-zeta STO, respectively.

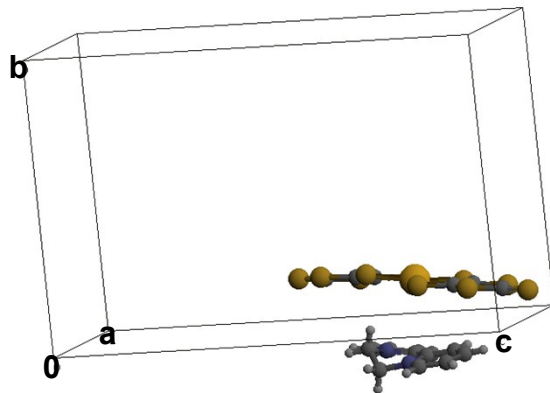


Figure S8. Interacting molecular pair in Table S6.

Table S6. Overlap (S) and transfer (H) integrals between $\text{Au}(\text{dmit})_2$ and BPY^a

T (K) and geometry ^b		LUMO-LUMO ^c	HOMO-HOMO	HOMO-LUMO	LUMO-HOMO
98 K, Au2A	S	-0.0012	-0.0015	-0.0065	0.0003
	H (eV)	0.0194	0.0292	0.1229	-0.0100
98 K, Au2B	S	-0.0038	0.0004	-0.0069	-0.0008
	H (eV)	0.0654	-0.0032	0.1271	0.0192
298 K, Au2A	S	0.0008	0.0010	-0.0058	0.0001
	H (eV)	-0.0127	-0.0187	0.1018	-0.0061
298 K, Au2B	S	-0.0020	-0.0002	0.0057	-0.0005
	H (eV)	0.0326	0.0005	0.1053	0.0133

^a For relative position of the molecular species, see Fig. S8.

^b The calculation was performed based on the atomic parameters obtained from the X-ray structural analysis at the temperature indicated. In the calculation, it was assumed that all the Au2 sites were occupied either by the square-planar coordinate Au(III) (Au2A) only or by the non-planar coordinate Au(III) (Au2B) only. Au2B is deviated toward the BPY considered in the calculation.

^c Interacting molecular orbital (MO) pairs are indicated as “MO of $\text{Au}(\text{dmit})_2$ - MO of BPY”. Here the singly occupied MOs (SOMOs) correspond to the HOMOs for $[\text{Au}(\text{dmit})_2]^{(1-q)-}$ and to the LUMOs for $\text{BPY}^{2(1-q)+}$ (q ; the amount of charge transfer).

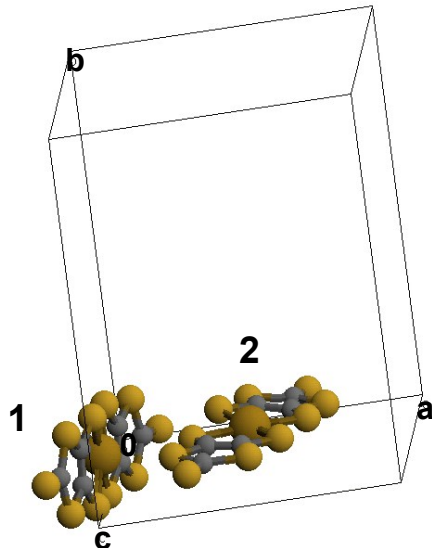


Figure S9. Interacting molecular pair in Table S7.

Table S7. Overlap (S) and transfer (H) integrals between the adjacent $\text{Au}(\text{dmit})_2^a$

T (K) and geometry ^b		LUMO-LUMO ^c	HOMO-HOMO	HOMO-LUMO	LUMO-HOMO
98 K, Au2A	S	0.0003	0.0008	-0.0012	0.0002
	H (eV)	-0.0092	-0.0182	0.0301	-0.0035
98 K, Au2B	S	-0.0003	-0.0008	0.0011	-0.0002
	H (eV)	0.0090	0.0177	-0.0286	0.0044
298 K, Au2A	S	-0.0001	-0.0001	0.0005	0.0003
	H (eV)	0.0022	0.0031	-0.0123	-0.0052
298 K, Au2B	S	0.0001	-0.0001	-0.0005	0.0003
	H (eV)	-0.0005	0.0028	0.0130	-0.0051

^a For relative position of the molecular species, see Fig. S9.

^b The calculation was performed based on the atomic parameters obtained from the X-ray structural analysis at the temperature indicated. In the calculation, it was assumed that all the Au2 sites were occupied either by the square-planar coordinate Au(III) (Au2A) only or by the non-planar coordinate Au(III) (Au2B) only.

^c Interacting molecular orbital (MO) pairs are indicated as “MO of $\text{Au}(\text{dmit})_2$ **1** - MO of $\text{Au}(\text{dmit})_2$ **2**”. Here the $\text{Au}(\text{dmit})_2$ **1** and **2** designate those in Fig. S9, respectively. The singly occupied MOs (SOMOs) correspond to the HOMOs for $[\text{Au}(\text{dmit})_2]^{(1-q)-}$ and to the LUMOs for $\text{BPY}^{2(1-q)+}$ (q ; the amount of charge transfer).

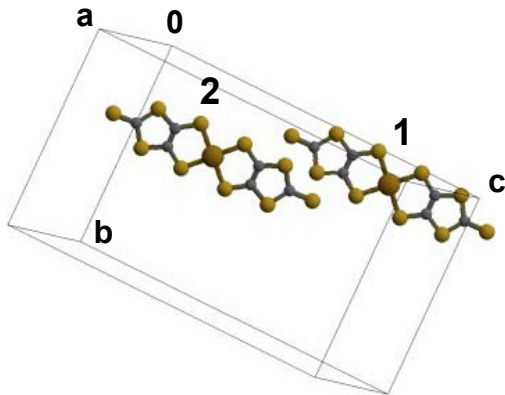


Figure S10. Interacting molecular pair in Table S8.

Table S8

Overlap (S) and transfer (H) integrals between the adjacent $\text{Au}(\text{dmit})_2^a$

T (K) and geometry ^b		LUMO-LUMO ^c	HOMO-HOMO	HOMO-LUMO	LUMO-HOMO
98 K, Au2A	S	0.0001	-0.0004	-0.0003	0.0003
	H (eV)	-0.0017	0.0099	0.0072	-0.0072
98 K, Au2B	S	0.0001	-0.0004	-0.0003	0.0003
	H (eV)	-0.0017	0.0099	0.0072	-0.0072
298 K, Au2A	S	0.0001	-0.0004	-0.0002	0.0003
	H (eV)	-0.0013	0.0098	0.0056	-0.0059
298 K, Au2B	S	0.0001	-0.0004	-0.0002	0.0003
	H (eV)	-0.0013	0.0098	0.0056	-0.0059

^a For relative position of the molecular species, see Fig. S10.

^b The calculation was performed based on the atomic parameters obtained from the X-ray structural analysis at the temperature indicated. In the calculation, it was assumed that all the Au2 sites were occupied either by the square-planar coordinate Au(III) (Au2A) only or by the non-planar coordinate Au(III) (Au2B) only.

^c Interacting molecular orbital (MO) pairs are indicated as “MO of $\text{Au}(\text{dmit})_2 \mathbf{1}$ - MO of $\text{Au}(\text{dmit})_2 \mathbf{2}$ ”. Here the $\text{Au}(\text{dmit})_2 \mathbf{1}$ and $\mathbf{2}$ designate those in Fig. S10, respectively. The singly occupied MOs (SOMOs) correspond to the HOMOs for $[\text{Au}(\text{dmit})_2]^{(1-q)-}$ and to the LUMOs for $\text{BPY}^{2(1-q)+}$ (q ; the amount of charge transfer).

4. Electrical resistivity

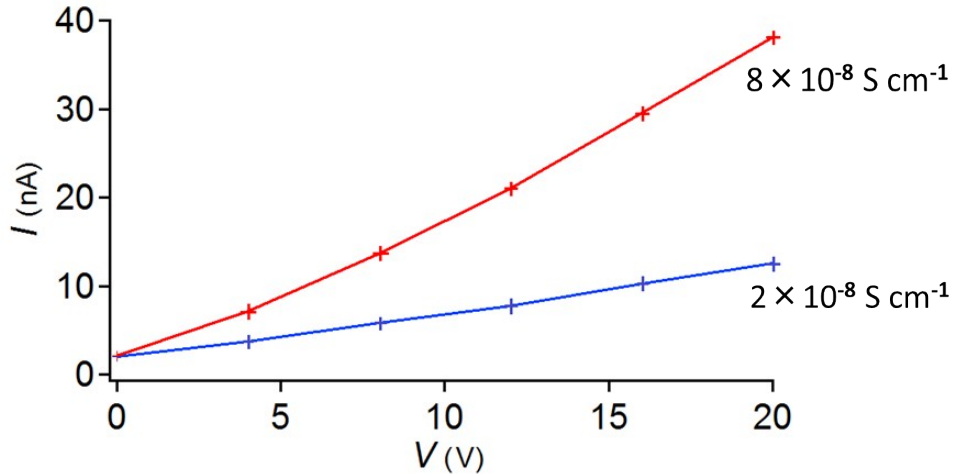


Figure S11. Electrical resistivity. Measured under dark (blue) and UV-irradiated (red) conditions, respectively (single crystal, //b, DC two-probe method) at 298 K. In actual measurement, a constant voltage V (-20 V < V < +20 V) was applied, and the resultant current I was measured. The data shown here was a typical steady state after several cycles (-20 V → -16 V → -12 V → -8 V → -4 V → 0 V → +4 V → +8 V → +12 V → +16 V → +20 V → -20 V → -16 V → ...), where some charge should have been stored at the interface of electrical contacts between sample and electrical leads. This explains why the I - V curve does not pass the origin. The observed response to UV (~250-450 nm; ~16-20 μWcm^{-2} at the crystal position) was reversible.

5. Magnetic susceptibility

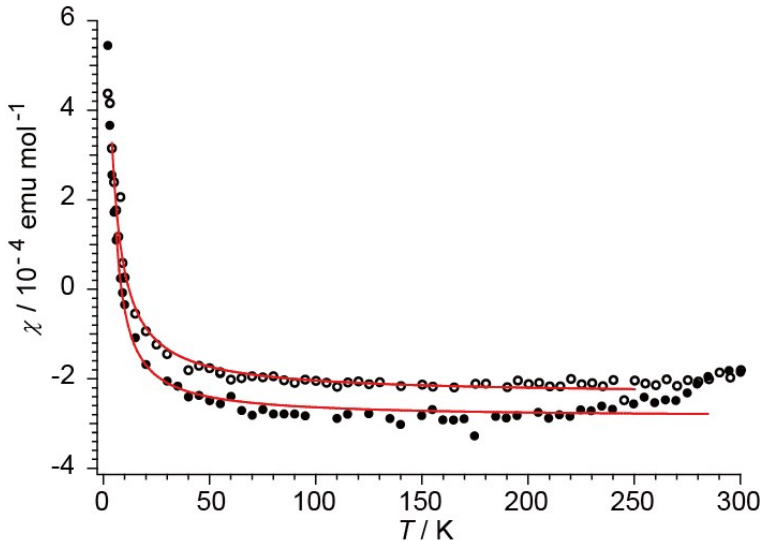


Figure S12. Curve-fitting analysis of magnetic susceptibility. Open (ZFC) and closed (FC) circles designate observed data (the same data in Fig. 5). Red curves are best-fitting curves by use of the following equation and parameters.

$$\chi = \frac{aC_0}{T - \theta} + \chi_{dia}$$

where χ , a , C_0 , T , θ and χ_{dia} designate magnetic susceptibility (emu mol⁻¹), an coefficient indicating the ratio of spins per a molar of BPY[Au(dmit)₂]₂, Curie constant of 1 molar spins (= 0.375 emu mol⁻¹K⁻¹), temperature (K), Weiss temperature (K), and diamagnetic susceptibility (emu mol⁻¹), respectively. Based on various fitting trials using different fitting data ranges and different initial parameters, typical best-fitting parameters are

$$a = 0.00887 \pm 0.00016$$

$$\theta/K = -1.888 \pm 0.070$$

$$\chi_{dia}/\text{emu mol}^{-1} = -(3.12 \pm 0.03) \times 10^{-4}$$

and

$$a = 0.00869 \pm 0.00066$$

$$\theta/K = -1.78 \pm 0.51$$

$$\chi_{dia}/\text{emu mol}^{-1} = -(2.36 \pm 0.04) \times 10^{-4}$$

for FC and ZFC data, respectively. These parameters imply that

$$a = 0.9 - 1.0 (\%)$$

$$\theta = -2 (K)$$

$$\chi_{dia} = -(2.5 - 3.0) \times 10^{-4} (\text{emu mol}^{-1})$$

Since most of the measurement temperature region ($2 \leq T \leq 300$ K) belongs to LT phase ($T_C \sim 280$ K), thus estimated parameters can be associated mainly with LT phase.

6. References

- S1. A. Altomare, G. Cascarano, C. Giacovazzo, A. Guagliardi, M. C. Burla, G. Polidori and M. Camalli, *J. Appl.*, 1994, **27**, 435.
- S2. R. H. Blessing, *Crystallography Reviews*, 1987, **1**, 3.
- S3. G. M. Sheldrick and T. R. Schneider, *Methods in enzymology*, 1997, **277**, 319.
- S4. Gaussian 09, Revision C.01, M. J. Frisch, G. W. Trucks, H. B. Schlegel, G. E. Scuseria, M. A. Robb, J. R. Cheeseman, G. Scalmani, V. Barone, G. A. Petersson, H. Nakatsuji, X. Li, M. Caricato, A. Marenich, J. Bloino, B. G. Janesko, R. Gomperts, B. Mennucci, H. P. Hratchian, J. V. Ortiz, A. F. Izmaylov, J. L. Sonnenberg, D. Williams-Young, F. Ding, F. Lipparini, F. Egidi, J. Goings, B. Peng, A. Petrone, T. Henderson, D. Ranasinghe, V. G. Zakrzewski, J. Gao, N. Rega, G. Zheng, W. Liang, M. Hada, M. Ehara, K. Toyota, R. Fukuda, J. Hasegawa, M. Ishida, T. Nakajima, Y. Honda, O. Kitao, H. Nakai, T. Vreven, K. Throssell, J. A. Montgomery, Jr., J. E. Peralta, F. Ogliaro, M. Bearpark, J. J. Heyd, E. Brothers, K. N. Kudin, V. N. Staroverov, T. Keith, R. Kobayashi, J. Normand, K. Raghavachari, A. Rendell, J. C. Burant, S. S. Iyengar, J. Tomasi, M. Cossi, J. M. Millam, M. Klene, C. Adamo, R. Cammi, J. W. Ochterski, R. L. Martin, K. Morokuma, O. Farkas, J. B. Foresman, and D. J. Fox, Gaussian, Inc., Wallingford CT, 2016.
- S5. GaussView, Version 5, R. Dennington, T. Keith and J. Millam, *Semicem Inc.*, Shawnee Mission KS, 2009.